SLAC-PUB-2828
October 1981
(A)

BEAM PARAMETER MEASUREMENTS FOR THE SLAC LINEAR COLLIDER*

J. E. Clendenin, C. Blocker, M. Breidenbach, T. N. Constant
R. J. Hollebeek, M. B. James, M. J. Lee, G. A Loew,
R. J. Miller, J. L. Siegrist, J. E. Spencer and J. B. Truher

Stanford Linear Accelerator Center
Stanford University, Stanford, California 94305

ABSTRACT

A stable, closely-controlled, high-intensity, single-bunch beam will be required for the SLAC Linear Collider. The characteristics of short-pulse, low-intensity beams in the SLAC linac have been studied. A new, high-intensity thermionic gun, subharmonic buncher and S-band buncher/accelerator section were installed recently at SLAC. With these components, up to 10^{11} electrons in a single S-band bunch are available for injection into the linac. The first 100-m accelerator sector has been modified to allow control of short-pulse beams by a model-driven computer program. Additional instrumentation, including a computerized energy analyzer and emittance monitor have been added at the end of the 100-m sector. The beam intensity, energy spectrum, emittance, charge distribution and the effect of wake fields in the first accelerator sector have been measured. The new source and beam control system will be described and the most recent results of the beam parameter measurements will be discussed.

I. INTRODUCTION

The Stanford Linear Collider (SLC) is a major project at the Stanford Linear Accelerator Center (SLAC) to reach an energy of 100 GeV in the center-of-mass within a few years. The existing 3 km linac is being upgraded to produce a high-quality, high-intensity, single-bunch beam with an energy of slightly more than 50 GeV for injection into a pair of collider arcs having an average radius of 300 m. The linac beam will consist of both a positron and and electron bunch accelerated within the same RF pulse of the linac. A dc magnet at the end of the linac will separate the two bunches into the two collider arcs. At the interaction region, where after half a turn the two arcs come together again, the beams will be focused to micron dimensions to improve luminosity. However, as the beams pass through each other they will undergo a high degree of disruption so that recovery of the beams after the collision will not be possible.

Linear colliders are a new class of accelerators that have been receiving increasing attention recently.[1] In a true collider, which consists of two linacs aimed at each other, the loss of RF power through synchrotron radiation is eliminated. Thus at some energy colliders, for which the cost scales linearly with the center-of-mass energy, $E_{c.m.}$, acquire a decided economic advantage over storage rings, whose cost scales as $E^2_{c.m.}$. To learn more about colliders, the SLC, in which a single linac is used, has been proposed.[2] The SLC design-energy, which is somewhat greater than the predicted mass of the neutral vector boson, Z^o, will permit an efficient investigation of the interaction of the electromagnetic and weak forces.

Although the 3-km electron accelerator at SLAC is the basis of the SLC, the requirements for the SLC beam are quite different from the properties of the present linac beams. The SLC-beam requirements are compared in Table I with the typical characteristics of the electron beam used to fill PEP. In addition to a 50% increase in the energy, it is seen that the beam must be confined to a single, very intense bunch with the conflicting requirement that the beam emittance be improved. Experience gained with linac operations in the past suggests that with charge densities of the magnitude proposed for the SLC, beam breakup can be avoided only by careful control of the beam while it is still at low energy.

With these problems in mind, the design and construction of a new injector was undertaken to produce the high-intensity single-bunch beams required for the SLC. In addition, the first 100 m of the linac (Sector 1) was modified to allow close control and monitoring of short-pulse beams in a manner similar to that which will be introduced eventually to all 30 linac sectors required for the SLC. This system and the beam tests which have been made using this system will be discribed.

TABLE I. SLC Beam Requirements

Parameter	Typical PEP Values	SLC Requirements
Number of bunches/pulse	3	1
Number of particles/bunch	10^9	$\geq 5 \times 10^{10}$
Transverse emittance area for electrons (π m_oc-cm)	0.06	$\leq$ 0.03
Energy spread at end of Sector 1		1%
Bunch length, σ_z (mm)	0.5	1
Injector jitter at 40 MeV		$\leq$ 1 G-cm
Energy gradient (MeV/m)	11.7	17

II. INJECTOR

As shown in Table I, the SLC requires an injector capable of producing $\sim 5 \times 10^{10}$ electrons in a single S-band bunch with a transverse emittance area on the order of 0.03 π m_oc-cm.

* Work supported by the Department of Energy, contract DE-AC03-76SF00515.

Invited paper presented at the 1981 Linear Accelerator Conference, Sante Fe, New Mexico, October 19-23, 1981.

A bunch length of $\sigma_z \sim 1$ mm is desirable, and the energy spread while not critical should be no more than one precent at the end of Sector 1.

Single-bunch beams have been available at SLAC for several years, but the intensity was limited to $\sim 10^9$ electrons per bunch.[3] Since the single bunches were selected by passing the regular linac gun-beams through a travelling-wave RF-chopper, the transverse emittance was quite poor. During the past year a new injector (CID) matching the characteristics desirable for the SLC has been installed at SLAC. As shown in Fig. 1, CID utilizes two resonant-cavity bunchers placed in series and operated at the 16th subharmonic of the linac accelerating frequency (2856 MHz) to compress the gun pulse sufficiently that the beam may then enter an S-band buncher and accelerator section.[4] The CID accelerator section and the identical section in the main linac injector are similar to the approximately 950 standard 3-m disk loaded waveguide (DLWG) sections which make up the linac. The two injector sections as well as the first three sections in Sector 1, which are driven by separate klystrons, each contribute ~40 MeV to the beam energy. The remainder of Sector 1 consists of repeated 4-section modules. Each module (girder), powered by a single klystron, contributes ~80 MeV (without SLED).

The CID gun must produce a very high-intensity, very narrow beam pulse. In addition, the gun must be capable of being pulsed twice during the period of the accelerating RF pulse. The second bunch will be directed to the positron target located near the high-energy and of the linac.

Two separate guns have been developed for CID -- a photoemission gun and a thermionic gun. The former operates on the principle of photoemission from a GaAs cathode activated by a Q-switched laser.[5] Polarized electron beams, which may prove important at high energy for the study of polarization-dependent effects, may be produced by using circularly polarized laser light of the correct frequency. Installation of the laser gun has been delayed pending improvements in the CID vacuum system.

The gun which has actually been used in CID is a new thermionic gun having a large diameter (1.5 cm) dispenser-cathode planar-grid assembly made by Eimac. The extremely small separation of the grid and cathode permits narrow gun pulses. The present avalanche-type pulser produces one 3-ns gun pulse during a single accelerating RF pulse. (A second generation pulser is under development to produce 1-ns gun pulses with full recovery on the order of 20 ns.) The new thermionic gun, which has been operated with CID for $\sim 10^3$ h with no significant difficulties, will produce peak currents of up to ~7 A at repetition rates of up to 180 pps.[6]

III. SECTOR 1

Earlier studies at SLAC with relatively low-intensity single-bunch beams made it clear that the transmission of high-intensity beams through the linac structure would be impossible unless the control system were vastly improved. The beam is affected by the fields generated by charged particles passing through the accelerating structure. These wake fields remain for a finite time after the passage of a particle so that an electron at a given axial position in the linac is affected by the resultant force due to the wake fields remaining from all electrons which previously passed the same position. The longitudinal forces, which increase the energy spread of the bunch, are generated by wake fields which simply

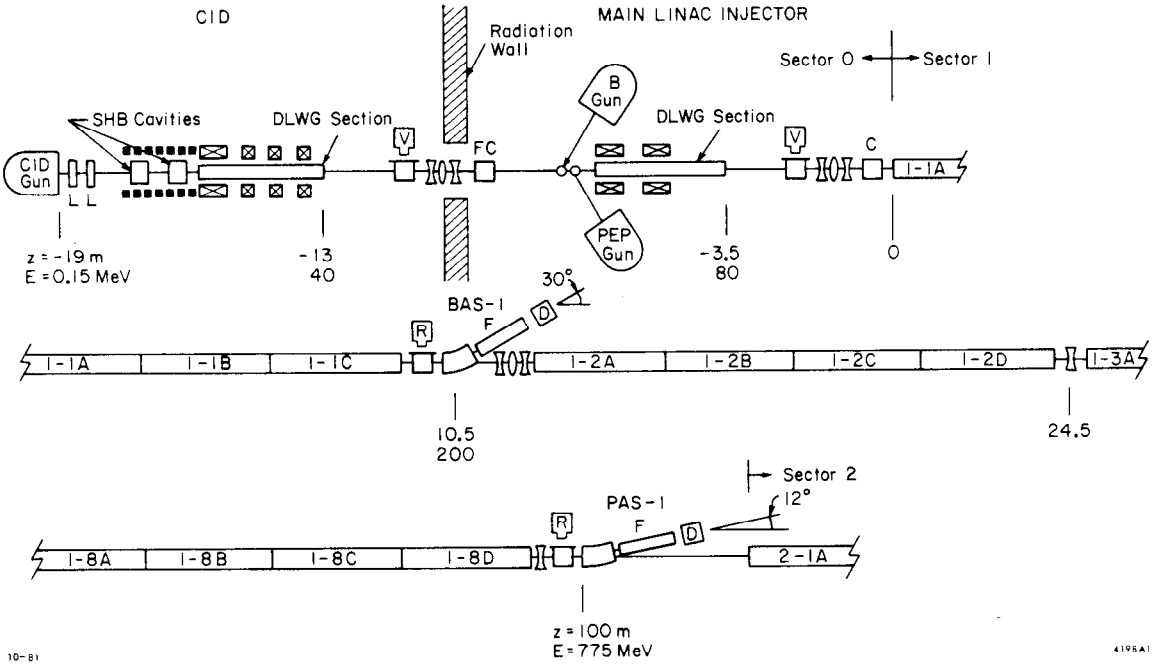

Fig. 1. General layout of Sectors 0 and 1, where L = lens, V = Vitecon camera, FC = Faraday cup, C = collimator, R = Reticon camera, F = SEM foils, and D = beam dump. Sector 1 consists of 8 girders, each (except girder 1-1) consisting of 4 identical 3-m sections of DLWG labeled A through D.

decrease with time, so that as a bunch is lengthened, electrons in the tail of the bunch are less affected by the longitudinal fields generated by electrons in the head. There is a similar beneficial effect when the separation of two bunches is increased.

The transverse forces are somewhat more complex. The strength of the transverse wake field depends on the displacement of the generation particle from the axis of the accelerating structure as well as the elapsed time since the passage of the generating particle. For a short time, on the order of 20 ps, the transverse wake fields, unlike the longitudinal fields, increase. Thus for the SLC beam in which $\sigma_z \sim 3$ ps, the transverse forces at the tail of the bunch are expected to be severe unless the beam can be kept on axis.

The present linac control system, in which the operator controls individual linac components with the aid of a mini-computer is inadequate for the SLC in several respects: the characteristics of the beam control devices are not well known; the beam must be tuned by a time-consuming trial-and-error method; and the beam monitoring is not precise enough or is totally insensitive to single-bunch beams. To overcome these problems the new computer control system will be model-driven, that is, the characteristics of each beam control device will be represented mathematically in the control program. A model for each control function -- focusing, orbit correction, emittance measurement, etc. -- will be an integral part of the control program. The control program will calculate on-line the needed values for the appropriate linac devices according to the control operation selected by the operator and display the predicted effect on the beam. Upon command the control program will set the calculated values in the appropriate linac devices. All critical beam parameters, such as transverse beam-position, will be continuously monitored.[7]

To implement this system in Sector 1, the quadrupoles, which are located at the short drift sections between 12-m girders, were calibrated and a standardization procedure established. Inside each quadrupole, integral with the drift tube connecting the two accelerator sections, new stripline position monitors were installed. Steering dipoles were also added at each quadrupole. The control computations as well as storage of data was accomplished in a central computer (VAX 11) connected to local CAMAC crates via a wide band cable system.

The magnet lattice was a FODO structure adjusted to minimize β^{max} in the following manner: knowing the emittance at the beginning of Sector 1, and temporarily neglecting the effects of acceleration, the strength of the quadrupoles in the first half of Sector 1 required to match the beam into a 90^o/cell configuration in the second half were computed on-line by the SLC control program. The resulting quadrupole strengths were then scaled by the correct energy. Such a solution is shown in Fig. 2(a) and (b). Once the quadrupole lattice was set, the beam orbit could be measured and the strengths of the dipole magnets required to center the beam computed and set.

Travelling-wave stripline beam position monitors were developed which fit inside a Sector 1 quadrupole as shown in Fig. 3. The four monitor strips are each ℓ = 12.5 cm long, grounded at their downstream end. The beam induced pulse read out at the upstream end of a strip is a doublet in which a leading negative pulse (for electrons) is followed $2\ell/c$ later by a positive pulse.[8] The pulses are stretched, combined into a single pulse with a dc restorer, and digitized. The digital

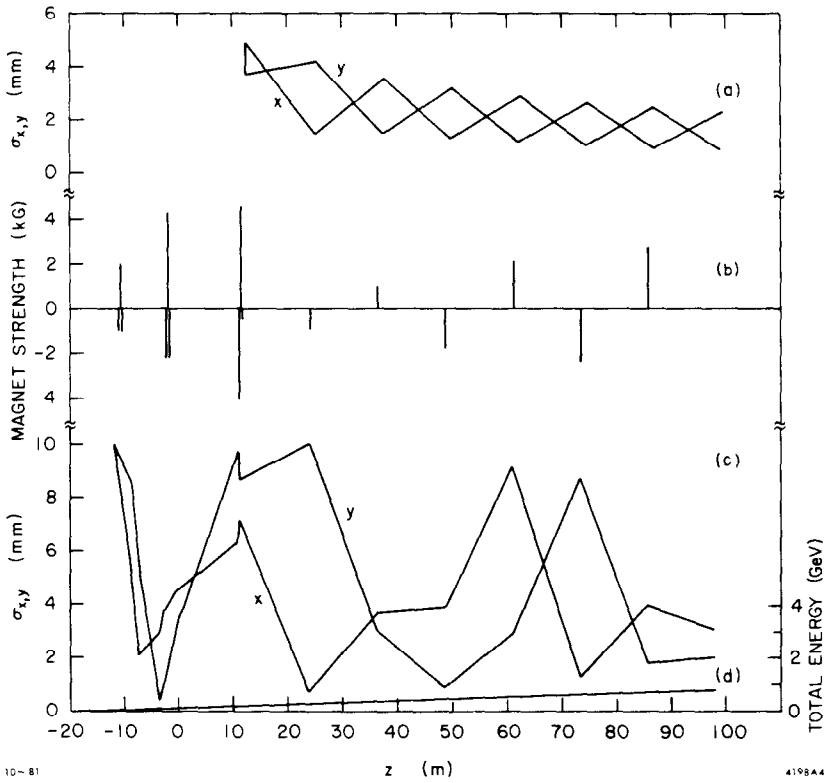

Fig. 2. A typical quadrupole configuration. The calculated beam radius, $\sigma_{x,y}$, in Sector 1 is shown in (a) for the magnetic strength (integrated gradient) in (b) which has been calculated to match a beam with a measured emittance area of 0.06 π m c-cm into a 90^o/cell FODO lattice. With the quadrupoles in Sector 0 empirically adjusted as shown in (b), the calculated radius is given in (c).

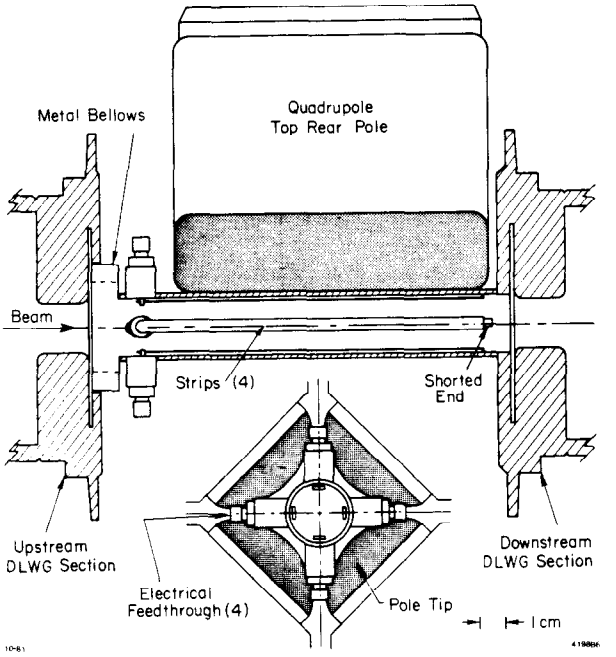

Fig. 3. Cross section of a stripline beam position monitor inside a quadrupole located between adjacent accelerator girders.

signal from each strip is read into the SLC program database. The transverse position of the beam is computed for each plane from the difference signal for two opposite strips, while the sum signal computed from all four strips is proportional to the beam intensity. The computed transverse position is designed to be accurate to within 0.1 mm.

An energy analyzer was installed at z = 10 m during the original construction of the linac. This analyzer consists of a 30° bending magnet and 12 SEM foils each with a resolution of 0.3%. Analog signals only are available from these foils.

More recently a new energy analyzer was installed at the end of Sector 1 having a 12° bend and 23, 0.3% foils plus one 0.1% foil. These foils are read out by a scanning ADC controlled by the SLC control program. The magnet supply was also under the control of the SLC program so that once enabled by the operator, the SLC program had complete control of energy analysis.

To compute an accurate transverse emittance, the control program must have access to a quantitative measure of the beam radius. For this purpose two new profile monitors were installed at z = 10 m and at z = 100 m respectively. These monitors had a standard SLAC CsI screen which could be inserted remotely. Each screen was viewed with a Reticon camera, an image digitizer which utilized a 32×32 array of photodiodes.[9] The image was displayed both locally on a TV screen and remotely in either video or graphic form via the SLC control program.

IV. BEAM PARAMETER MEASUREMENTS

The parameters of the new high-intensity single-bunch beam that have been measured include the beam emittance, intensity, transmission, and the effects of transverse deflecting fields.

The transverse emittance of the beam was found by measuring the beam radius at a Reticon profile monitor for several orientations of the beam phase space ellipse. The ellipse was rotated by the control program by changing the strength k (integrated gradient/beam rigidity) of one of the upstream quadrupoles. If the behavior of the beam at the profile monitor is represented by the beam sigma matrix,[10] $\sigma(k)$, then $\sigma_{11}(k)$, the square of the beam radius, describes a parabola,

$$\sigma_{11}(k) - \sigma_{11}(k_o) = M_{12}^2 \, C \, (k-k_o)^2 \quad ,$$

in which k_o is the quadrupole strength for the minimum spot size at the monitor, M_{12} is an element of the matrix for the transport of the beam between the quadrupole and the monitor,[10] and C is a constant. Since $\sigma_{11}(k_o)$ and C can be found from a parabolic fit to the data, the transverse emittance, ε_x, can be computed by the control program from the expression

$$\varepsilon_x \equiv \sqrt{\sigma_{11}\sigma_{22} - \sigma_{21}^2} = \frac{\sigma_{11}(k_o)\, C}{M_{12}^2} \quad ,$$

where M_{12} is know theoretically. In these expressions the x and y motions are assumed to be decoupled and ε_y can be found by substituting the σ subscripts 3,4 for 1,2. An example of a set of curve fits for a relatively low intensity beam ($\sim 5\times10^9$ electrons/bunch) is shown in Fig. 4. The emittance area calculated from these curves is $\pi\varepsilon_x = 0.02\ \pi\ m_o c\text{-cm}$ and $\pi\varepsilon_y = 0.009\ \pi\ m_o c\text{-cm}$. The emittance at higher beam intensities was not

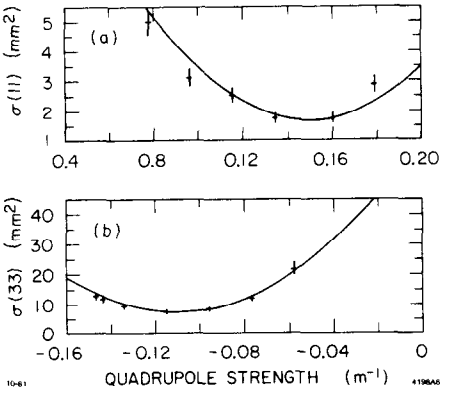

Fig. 4. Parabolic fit to beam spot size (sigma matrix element) plotted as function of quadrupole strength (integrated gradient/beam rigidity) in (a) horizontal and (b) vertical planes at z = 100 m.

measured although under the existing control conditions it was clearly larger.

The energy and energy spread was measured at the end of Sector 1 with the new 12° energy analyzer. The energy spread, shown in Fig. 5, was typically about 2 foils wide or $\Delta E/E \sim 0.6\%$ at 770 MeV.

A single foil from this same analyzer was used to determine the longitudinal charge distribution. The analyzed current, $dq/d\gamma$, was measured as a function of the phase, ϕ, of the klystron immediately upstream. Two spectra were observed 180° apart from which the charge distribution could be deduced according to the following expression:[11]

$$\frac{dq}{d\theta} = \frac{(dq_a/d\gamma)(dq_b/d\gamma)\ \gamma_1\ 2 \sin \frac{1}{2}(\phi_b - \phi_a)}{|dq_a/d\gamma| + |dq_b/d\gamma|} ,$$

where θ is the beam phase and γ_1 is the peak energy contribution of the analyzing klystron. The charge distribution shown in Fig. 6 was calculated by assuming the peaks of the two measured spectra correspond to the same θ, and that points at the same percentage of the peak value represent nearly the same θ. For the SLC beam at low intensities, σ_z is on the order of 1 mm, a factor of 2 greater than typical SLAC linear beams.

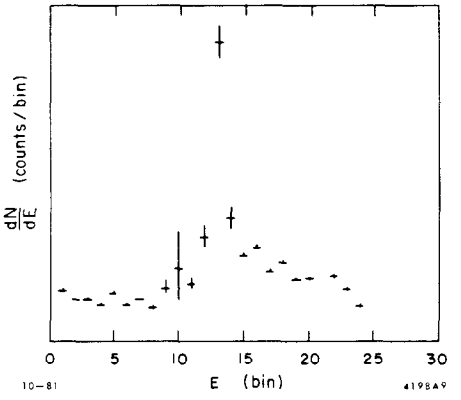

Fig. 5. Typical scan of the 24 SEM foils at the energy analyzer at z=100 m. Each bin represents a foil for which $\Delta E/E = 0.3\%$. The magnet current corresponded to a beam energy of 770 MeV at the center foil.

The beam intensity was measured in several ways. At the beginning and end of Sector 1 are located toroids with which the charge in a linac beam pulse can be measured with an accuracy of ±10%. Since the SLC pulse contains about the same charge as a standard 1.6 μs linac beam pulse, these toroids are excellent standards although their locations are limited and in addition they cannot distinguish between single- and multiple-bunch beams.

This latter problem is solved by monitoring the beam induced pulse at a ceramic gap in the beam pipe. By reducing the resistance across a short gap to $< 10\ \Omega$ the rise time of the induced pulse was kept below 100 ps. Ceramic gaps were installed at the z = -16, -10, +10, and +100 m locations. A typical signal observed at the z = -10 m location using a sampling scope with a

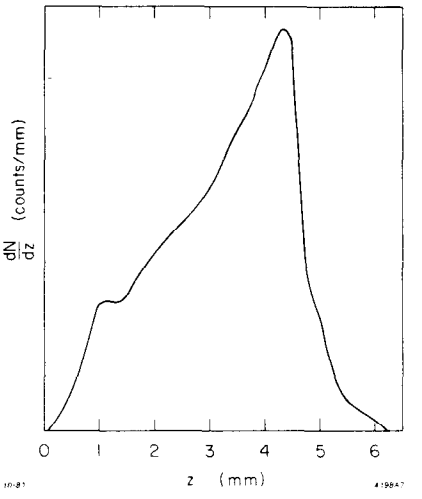

Fig. 6. Longitudinal charge distribution measured for the beam profile shown in Fig. 9.

100 ps rise time and connected to the gap monitor via a high-quality air-dielectric coaxial cable is shown in Fig. 7. The unfortunate tendancy of these monitors to ring at S-band frequencies somewhat complicates the measurement, but by varying the timing of the gun pulse relative to the subharmonic buncher RF to create first a pre-bunch and then a post-bunch, it was possible to determine that the beam pulse did indeed contain but a single S-band bunch. The gain of the gap monitors was calibrated in the laboratory and so provided an independent measure of the beam intensity.

A third type of intensity monitor, which solved the problem of proper location, was the stripline beam position monitor described earlier. These monitors provided an accurate although not absolute measurement of intensity at each quadrupole location for the SLC control program.

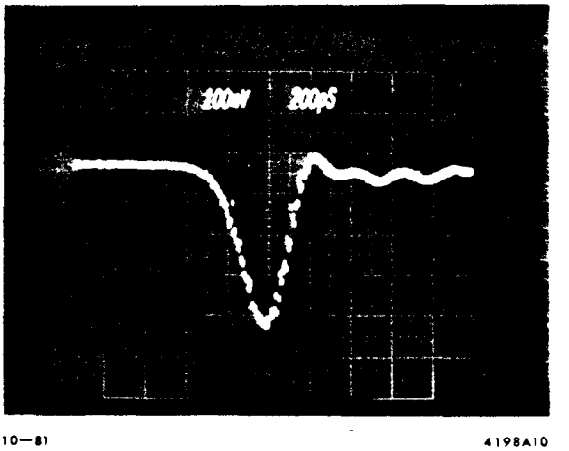

Fig. 7. Sampling scope display of the single-bunch beam signal from the gap monitor located at z = -10 m. The scope risetime was slightly better than 100 ps. The charge in the bunch was ~ 1 nC.

An absolute measure of beam current was possible at z=-9 m with an insertable Faraday cup.

With CID it was possible to produce over 10^{11} electrons (> 16 nC) in a single S-band bunch,[12] which is approximately two orders of magnitude greater intensity than previous single-bunch beams at SLAC and perhaps an order of magnitude greater charge than reported elsewhere.[13-14]

To prevent emittance growth due to the large space charge forces present in the CID beam, the gun was biased at 150 kV and the beam energy was increased as rapidly as possible. Up to 40 MeV the beam radius was confined by a series of manually controlled lenses and solenoids. Between CID and Sector 1, the magnet lattice, consisting of a quadrupole triplet on either side of the main injector solenoid, approximated a periodic array with a 3-m interval. The two triplets were adjusted through the SLC control program, but the transport of the beam to Sector 1 was not modeled. Instead the strength of each focusing element was adjusted to give a betatron phase shift of 90° per period by maximizing the transmission through the succeeding element.

The modeling for Sector 1 began at z = 11 m where the third quadrupole triplet shown in Fig. 1 was located. This triplet was generally operated as a doublet to improve the match into the Sector 1 lattice. Post-experiment analysis has shown that a match was never in fact achieved Fig. 2(b) and (c) shows a typical result where the quadrupole configuration for Sector 1 was identical with that for Fig. 2(a).

The matching was unlikely to succeed since the emittance at the beginning of Sector 1 was calculated from the emittance measured at z = 100 m. The task of efficiently transporting the beam to Sector 1 was also difficult because of a limiting orifice[15] of r = 4.9 mm (a collimator) located at z ~ 0. To get the beam through this aperture, it appears that a great deal of scraping was experienced in the vicinity of both the first and third triplets. Since about half the charge is at a radius > $\sigma_{x,y}$, the observed transmission through the injector region which is indicated in Fig. 8 (curve a) to be ~50% is consistent with the known operating conditions.

Even with the poor match in Sector 1, the effectiveness of the SLC control program is illustrated by the high transmission shown for this region in curve b of Fig. 8. However, when the current in Sector 1 increased above about 1.5×10^{10} electrons/bunch, wake field effects became a limiting factor. As the current increased unstable "arms" were extended from the main beam profile observed at the end of the Sector. At the highest intensities the entire profile appeared to be unstable.

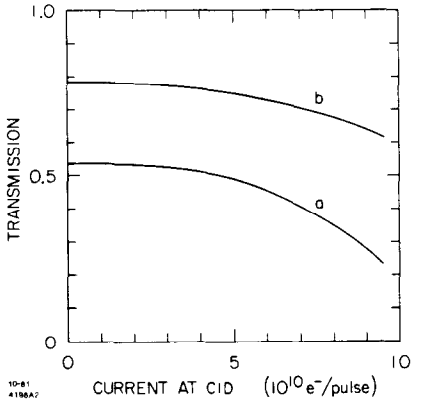

Fig. 8. Beam transmission as a function of current at output of CID (see Ref. 12). Curve a is for Sector 0 only, curve b is for Sector 1 only.

To study the transverse wake fields under more controlled conditions, the intensity was reduced to ~10^9 electrons/bunch, a level for which the beam was fairly stable through Sector 1. The beam was then allowed to drift for the last 50 m -- equivalent to approximately 180° of betatron phase advance -- of the Sector. Using the dipole corrector magnets located in this region, the drifting beam was given known offsets between ±2 mm (confirmed with the position monitors), and then recentered at the end of the Sector. The wake fields generated by the off-centered beam displaced the tail of the bunch relative to the head. The displacement was observed as a shift in portions of the beam profile at the end of the Sector. A comparison of the profile in the horizontal plane (summed over the vertical plane) for horizontal displacements of 0 and of ±2 mm are shown in Fig. 9(a), (b) and (c).

The beam profile at the end of Sector 1 for a zero emittance beam can be computed for any assumed wake function using a model of the linac and a given longitudinal charge distribution. The results of such a computation by R. Stiening, using the measured charge distribution (Fig. 6) corresponding to the data of Fig. 9, and with the undeflected beam profile of Fig. 9(a) folded in, is shown in Fig. 9 for three assumed values of the wake function. The wake function was calculated by P. B. Wilson and K. Bane from a modal analysis[16] of the SLAC accelerating structure with analytic extension. In Fig. 9(d), (e) and (f), a weight of 0.5, 1.0 and 2.0 was assigned to the calculated wake function. Clearly the computed profile of Fig. 9(e) is most like the measured profiles of Fig. 9(b) and (c). This result suggests the computed transverse wake function is correct within a factor of 2.

V. CONCLUSIONS

As the beam intensity was increased, it was evident that the emittance increased beyond the desired level. Since the effects of wake fields measured at low intensities agreed with the computed effects, it seems that the conditions for beam injection were not optimized. The most likely source of the problem would be an unstable power supply for one of the injector dipole orbit correctors -- indeed a post-experiment check of all CID power supplies revealed a likely candidate. The inclusion of the CID corrector power supplies in the SLC control program will help eliminate this problem.

To achieve the maximum possible transmission, a model must be developed for the transport of the beam from CID to Sector 1. Control of the beam would also be improved by the addition of a new quadrupole triplet at the exit of the CID DLWG-section.

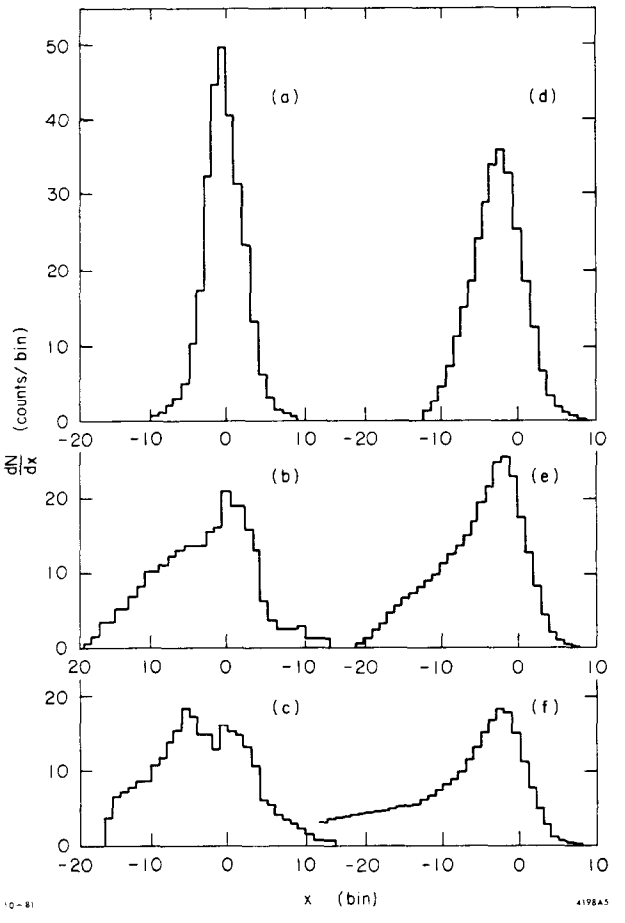

Fig. 9. Beam profiles in the horizontal plane (32 bins/cm): measured profiles with beam offset of (a) 0, (b) +2 mm, and (c) -2 mm; computed profiles for an offset of -2 mm using a computed wake function with a weight of (d) 0.5, (e) 1.0, and (f) 2.0. All profiles are integrated over the vertical plane and have normalized areas. Note the reversed abscissa in (b).

The SLC beam tests in Sector 1 will continue during the present linac operating cycle. With the improvements just described it should be possible to increase in a controlled manner the beam intensity transmitted through Sector 1.

REFERENCES

1. Summarized in U. Amaldi, Proceedings of the IXth International Symposium on Lepton and Photon Interactions, Fermilab (1979), p. 314.
2. SLAC Linear Collider Conceptual Design Report, SLAC-229 (1980); B. Richter, R. A. Bell, K. L. Brown et al., Proceedings of the XIth International Conference on High-Energy Accelerators, CERN (1980), p. 168.
3. J. E. Clendenin, G. A. Loew, R. H. Miller et al., IEEE Trans. Nucl. Sci. NS-28, 2452 (1981).
4. M. B. James and R. H. Miller, IEEE Trans. Nucl. Sci. NS-28, 3461 (1981).
5. C. K. Sinclair and R. H. Miller, IEEE Trans. Nucl. Sci. NS-28, 2649 (1981).
6. Anode currents of 20 A have been produced with a different pulser. See R. F. Koontz, "CID Thermionic Gun System," this conference.
7. M. J. Lee, C. Blocker, A. W. Chao et al., IEEE Trans. Nucl. Sci. NS-28, 2155 (1981).
8. J.-L. Pellegrin, Proceedings of the XIth International Conference on High-Energy Accelerators, CERN (1980), p. 459.
9. The Reticon camera system is described in B. Gottschalk, SLAC-TN-81-7 (1981).
10. K. L. Brown, F. Rothacker, D. C. Carey and Ch. Iselin, TRANSPORT, SLAC-91 (Revision 2) and UC-28 (1977).
11. G. Mavrogenes, M. B. James, R. F. Koontz and R. H. Miller, Proceedings of the XIth International Conference on High-Energy Accelerators, CERN (1980), p. 481.
12. The current measured at the Faraday cup at z = -9 m and at the gap monitor at z = -10 m was used as the basis for the source current since this location was far enough away from the buncher to be unaffected by the unbunched electrons. However the computed transmission from CID may be unduly low since it is based on the intensity measured by a beam position monitor located near CID at z = -13 m.
13. J. Tanaka, I. Sato, S. Anami et al., Proceedings of the 1979 Linear Accelerator Conference, BNL51134 (1979), p. 319.
14. Up to 40 nC in a single bunch has been produced with the L-band linac at ANL using a new double-cavity buncher operated at the 12th subharmonic, although the useful charge is generally limited to 25 nC. G. Mavrogenes, ANL, private communication.
15. Although the accelerator drift sections have a radius of ~12 mm, the limiting aperture within each 3-m DLWG section has a radius of ~8.7 mm.
16. The analysis made use of the computer program TRANS for finding the modes in the structure as described in B. Zotter and K. Bane, PEP-NOTE-308 (1979).